Organic Homojunction Diodes with a High Built-in Potential: Interpretation of the Current-Voltage Characteristics by a Generalized Einstein Relation

K. Harada,[1] A. G. Werner,[1] M. Pfeiffer,[1] C. J. Bloom,[2] C. M. Elliott,[2] and K. Leo[1]
[1]*Institut für Angewandte Photophysik, Technische Universität Dresden, 01062 Dresden, Germany*
[2]*Chemistry Department, Colorado State University, Fort Collins, Colorado 80523, USA*

(Received 11 February 2004; published 24 January 2005)

We realize *p*- and *n*-type doping of the organic semiconductor zinc-phthalocyanine using a novel strong organic donor. This allows us to demonstrate the first stable and reproducible organic *p*-*n* homojunctions. The diodes show very high built-in potentials, attractive, e.g., for organic solar cells. However, the diode characteristics cannot be described by the standard Shockley theory of the *p*-*n* junction since the ideality factor strongly increases with decreasing temperature. We show that this behavior can be explained by deviations from the Einstein relation for disordered materials.

DOI: 10.1103/PhysRevLett.94.036601 PACS numbers: 72.80.Le, 73.40.Lq, 73.40.Qv, 82.45.Aa

Organic semiconductors are of high interest due their suitability for novel applications such as organic light emitting diodes (OLED) and organic solar cells. Surprisingly, a prerequisite for all inorganic semiconductor devices, the controlled doping to achieve *n*- and *p*-type conductivity, has only occasionally been addressed in organic semiconductors [1–3]. Despite some attempts with electrochemical systems [4], in which no relevant diode rectification was obtained, no stable and reproducible *p*-*n* homojunction (being the archetype of semiconductor devices) has been reported for organic semiconductors. In particular, it has not yet been possible to investigate whether such an organic *p*-*n* junction follows the standard Shockley model [5]. For semiconductor junctions based on amorphous silicon, deviations from the Shockley model due to recombination at defects in the intrinsic layer distributed in energy and space [6] have been reported.

Since organic semiconductors are usually characterized by high levels of disorder and hopping transport, it will be interesting to determine whether the Shockley theory is obeyed in these systems. The interest in the organic *p*-*n* homojunction is also spurred by the fact that organic devices with superior properties [7], including OLED with the highest efficiencies reported yet [8], have recently been prepared with organic *p*-*i*-*n* heterojunctions.

In this Letter, we present the first realization of a stable organic *p*-*n* homojunction. With an intrinsic interlayer, the junction exhibits excellent blocking behavior and a high built-in potential attractive for applications. The current-voltage relation significantly deviates from Shockley theory. We show that the results can be explained by diffusion theory taking into account the disorder inherently present in organic thin films.

The challenge in realizing an organic *p*-*n* homojunction lies in the energetics of the dopant molecules: For *p*-type doping, it is necessary to find a molecule where the lowest unoccupied orbital (LUMO) is energetically located near or below the highest occupied molecular orbital (HOMO) of the organic semiconductor host (see Fig. 1). For *n*-type doping, the HOMO of the dopant molecule has to be energetically near or above the LUMO of the semiconductor host. It is obvious that, for doping the same matrix with both *n*- and *p*-type dopants, one needs dopant molecules which have very high and low lying orbitals, respectively. For this reason, it is much easier to realize a *p*-*n* heterojunction where the two different host materials are chosen in a way that the energy difference between the LUMO of the *n* host and the HOMO of the *p* host is small.

Efficient *p*-type doping of various organic hole transport materials including zinc-phthalocyanine (ZnPc) has been studied already in detail [2,3]. The doping leads to quite high carrier concentrations of up to 10^{20} cm^{-3}. In contrast, *n*-type doping of electron transport layers using organic donors has been achieved only recently [9]. Bloom *et al.* [10] have demonstrated that the electrochemically reduced form of the transition metal complex bis(terpyridine)ruthenium(II) ($[\mathrm{Ru(terpy)_2}]^0$) can be a promising electron-injecting cathode material in OLED's due to its low work function. The oxidation potential of $[\mathrm{Ru(terpy)_2}]^0$ is as low as -1.7 V vs Ag/Ag$^+$ [11,12].

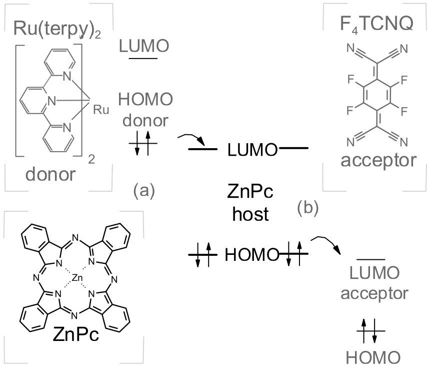

FIG. 1. Energy level scheme of *n*-type (a) and *p*-type (b) doping.

We have chosen ZnPc as the matrix of our diodes because its reduction potential of approximately -0.93 V vs saturated calomel reference electrode (approximately -0.9 V vs $\mathrm{Ag/Ag^+}$) [13] should allow an electron transfer from the donor $[\mathrm{Ru(terpy)_2}]^0$. Furthermore, the properties of *p*-type ZnPc (*p*-ZnPc) layers doped with tetrafluoro-tetracyano-quinodimethane ($\mathrm{F_4}$-TCNQ) are well investigated.

The donor compound $[\mathrm{Ru(terpy)_2}]^0$ was synthesized in its 2+ oxidation state and electrochemically reduced [10]; $\mathrm{F_4}$-TCNQ (Acros Organics) is used as provided. The matrix material ZnPc (Syntec GmbH) was purified by vacuum gradient sublimation. The indium tin oxide (ITO) coated glass substrates (Thin Film Devices Inc., sheet resistance $<80\ \Omega/\square$) are cleaned by ultrasonic treatment in acetone and ethanol, rinsed in deionized water and treated with ozone plasma. Matrices and dopants are coevaporated from ceramic crucibles in a UHV chamber. All handling of $[\mathrm{Ru(terpy)_2}]^0$ was carried out in an inert atmosphere. The measurements were conducted in vacuum.

First, we briefly discuss the electrical properties of ZnPc films doped with the *n*-type dopant $[\mathrm{Ru(terpy)_2}]^0$. For a molar doping ratio of 1:35, we achieve conductivities of 2.7×10^{-6} S/cm at room temperature. The conductivity increases superlinearly with the doping ratio, indicating shallow donor states according to the model of Maennig *et al.* [3]. Field-effect measurements confirm *n*-type conduction of the ZnPc films.

Because of the doping ratio mentioned, the diodes require an undoped *i* layer between *p* and *n* layers to enable good rectification: the space-charge region of the *p*-*n* junction would be only a few nm thick and easily tunneled through [14]. The *p*-*i*-*n* homojunction is thus formed from three ZnPc layers: *p*-ZnPc/*i*-ZnPc/*n*-ZnPc with ITO and Al Ohmic contacts, respectively. For comparison, we have also realized a Schottky junction: The *M*-*i*-*n* diode consists of ITO/*i*-ZnPc/*n*-ZnPc. The parameters of these junctions are summarized in Table I, and the schematics are depicted as insets in Fig. 2(a).

Capacitance-voltage (*C*-*V*) spectroscopy allows the determination of the built-in potential V_{bi} of the diodes. The capacitance of a diode is characterized by the width of the depletion layer, which is a function of the applied bias voltage *V*. The application of a forward bias reduces the width of the space-charge region. When *V* reaches V_{bi}, the space-charge region disappears. Figure 2(a) shows the *C*-*V* spectra of the two types of junctions. A collapse of the capacitance is observed for both samples when the applied voltage exceeds 0.8 V. This means that the *p*-*i*-*n* and *M*-*i*-*n* diodes have a built-in potential of $\cong 0.8$ V at room temperature, noticeably higher than doped organic heterojunction solar cells [15] consisting of ZnPc and fullerene $\mathrm{C_{60}}$.

TABLE I. Doping ratios and layer thicknesses of the diodes.

	Doping ratio/thickness of layer		
Type of junction	*p*-ZnPc	*i*-ZnPc	*n*-ZnPc
p-*i*-*n* homo	1:38/15 nm	$-$/30 nm	1:46/40 nm
M-*i*-*n*		$-$/50 nm	1:41/100 nm

Additionally, we changed the Al top contact to Au, which did not affect the current-voltage (*I*-*V*) characteristics; in particular, V_{bi} remained unchanged. Since the work function difference of the ITO/Au couple is much smaller and even opposite in sign to the ITO/Al pair, it is not the contact pair but, indeed, the Fermi levels of the *p* and the *n* layers that are responsible for the built-in potential. Au obviously forms an Ohmic contact with *n*-ZnPc.

Further, we varied the *i* layer thickness to 60 and 90 nm, respectively. No change in the current density is observed

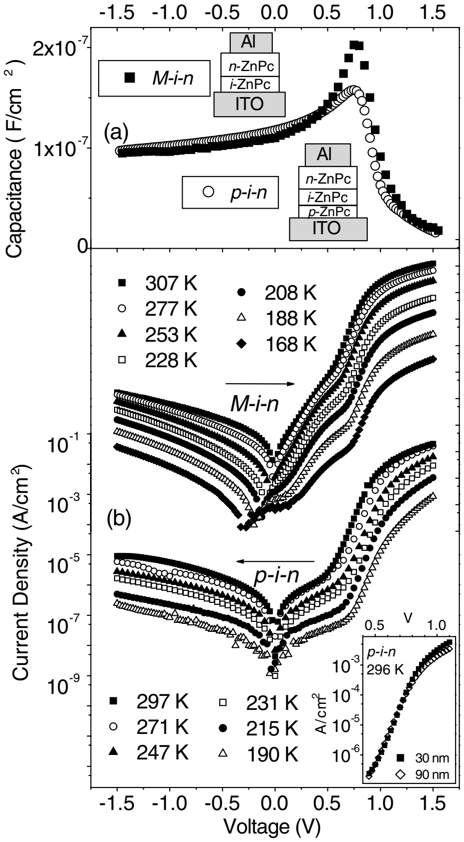

FIG. 2. (a) *C*-*V* spectra of the *M*-*i*-*n* homojunction (■) measured at 2 kHz and *p*-*i*-*n* junction (○) measured at 3 kHz. Insets depict the schematics of both *p*-*i*-*n* and *M*-*i*-*n* samples. (b) *I*-*V* characteristics of *M*-*i*-*n* junction and *p*-*i*-*n* homojunction (*i* thickness 30 nm) at various temperatures. Through the measurement periods, e.g., three weeks, the samples in vacuum (sometimes kept in an $\mathrm{N_2}$ atmosphere) repeatedly exhibited the same *I*-*V* curves at each temperature, while the diode properties were lost rapidly in air due to the oxidation of the *n* dopant. The linear part above 0.5 V reflects the junction, while the characteristics are controlled by an inevitable shunt resistance below 0.5 V. Inset: *I*-*V* characteristics of *p*-*i*-*n* samples with the *i* thicknesses of 30 nm (■) and 90 nm (◇) at room temperature.

in the exponential region (only in the bulk limited part above V_{bi}; see the inset of Fig. 2(b)]. Hence, we can rule out the influence of space-charge limited currents or field-dependent mobilities mimicking diodelike characteristics below the built-in potential.

We thus apply the general diode equation

$$J = J_0\left[\exp\left(\frac{qV}{nkT}\right) - 1\right], \tag{1}$$

which describes the *I*-*V* characteristics of both *p*-*n* junctions and Schottky diodes. J_0 refers to the saturation current, V the applied voltage, k the Boltzmann constant, T the temperature, and n the so-called ideality factor. n is unity in the Shockley theory for *p*-*n* junctions in the absence of recombination, as well as for thermionic emission theory and diffusion theory for Schottky diodes. The ideality factor and the saturation current can be obtained from the slope and the intercept, respectively, obtained by extrapolation of the linear part of the semilogarithmic plot of J vs V. Figure 2(b) shows the temperature dependence of *I*-*V* plots from the *p*-*i*-*n* homojunctions and the *M*-*i*-*n* junction.

It is immediately obvious from Fig. 2(b) that the standard diode equation with a temperature-independent n does not describe our data since the slopes of the linear parts of the semilogarithmic *I*-*V* plots depend only weakly on temperature. This behavior indicates that n increases when the thermal energy kT decreases. From Eq. (1), $n = \frac{kT}{q}\frac{\partial \ln J}{\partial V}$ for $qV \gg nkT$. The n factors of our *p*-*i*-*n* and *M*-*i*-*n* samples at room temperature are $n = 1.8$–2.0. For decreasing temperature, the value of n strongly increases [Fig. 3(a)].

The deviation from the Schottky theory for the *M*-*i*-*n* is also obvious from another experimental finding. The diffusion theory is applicable to describe the saturation current in low-mobility Schottky diodes [16]. The effect of electron collisions within the depletion region is included in this theory. Assuming that the thickness of the i layer is very large compared to the expansion of the depletion layer due to the bias voltage V, the expression of the saturation current J_0 [16] can be simplified using a prefactor Σ_0 with the dimension of conductivity:

$$J_0 = \Sigma_0 \frac{q}{kT}\exp\left(-\frac{q\Phi_B}{kT}\right), \tag{2}$$

where Φ_B denotes the Schottky barrier height. One can estimate the Schottky barrier height of the *M*-*i*-*n* diode by the fitting of saturation currents at various temperatures [Fig. 3(b)]. The value from the best fit curve is $\Phi_B = 0.34$ V, i.e., much lower than the $V_{\mathrm{bi}} \cong 0.80$ V obtained from the *C*-*V* plot, which is opposite the expectation. The saturation current of the *p*-*i*-*n* diode exhibits a temperature dependence similar to the *M*-*i*-*n* junction [Fig. 3(b)].

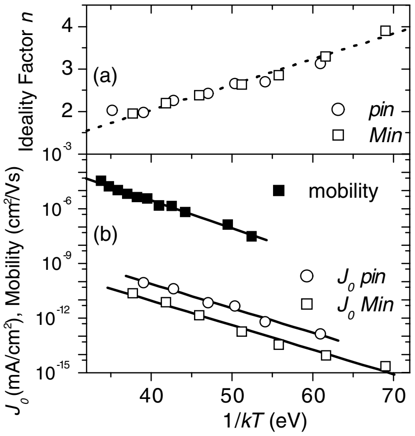

FIG. 3. Temperature dependence of (a) the ideality factors n and (b) the saturation current J_0 of *p*-*i*-*n* and *M*-*i*-*n* samples. For comparison, in (b) the field-effect mobility of a Ru(terpy)$_2$: ZnPc (1:41) layer is given.

We now present a simple model that could quantitatively explain the experimental observations: In principle, each *I*-*V* curve of our diodes can be described either by Shockley or by diffusion theory. However, the temperature dependence of the diode parameters does not follow the classical models: the ideality factor n does not obey the $1/kT$ rule, and the saturation current J_0 does not reflect the built-in potential. In the Shockley theory for *p*-*n* junctions, the presence of the local field is neglected for the derivation of the current equation. The diffusion theory discussed below for the *M*-*i*-*n* characteristics takes the local field in the i layer into account. In order to explain our experimental results, we need to modify the diffusion theory. The property of the *p*-*i*-*n* sample with a thick i layer would be described in virtually the same way as the *M*-*i*-*n* sample using the diffusion theory, as it is indicated by the nearly identical behavior of n and J_0 (see Fig. 3).

In the following, we show that the temperature dependence of the ideality factor and the low barrier height obtained from the *I*-*V* plot can be explained in the first approximation by considering deviations from the Einstein relation in disordered systems. In diffusion theory, drift and diffusion currents of the *M*-*i*-*n* diode [16]

$$J = q\left[n_e \mu \frac{\partial V}{\partial x} + D\frac{\partial n_e}{\partial x}\right] \tag{3}$$

are considered. Here, μ denotes the charge carrier mobility and n_e the charge density. The Einstein relation can be applied to replace either μ or D. In the classical formulation $\frac{qD}{\mu} = kT$, which is derived for nondegenerate systems in thermal equilibrium [17]. However, it has been shown that deviations from the classical Einstein relation occur for transport under equilibrium [18] and nonequilibrium [19] conditions in disordered materials. To account for that, we now temporarily let $qD/\mu = f(T)$, where $f(T)$ is some unknown function of temperature. The further considerations are analogous to the classical derivation [16]. An integrating factor $\exp[-qV/f(T)]$ can be used to integrate Eq. (3) over the i layer ranging from $x = 0$ to W, assuming the mobility and $f(T)$ to be spatially constant:

$$J \int_0^W \exp\left[-\frac{qV}{f(T)}\right] dx = \mu f(T) \left\{ n_e \exp\left[-\frac{qV}{f(T)}\right] \right\}_0^W. \quad (4)$$

The boundary conditions are $V(0) = -(V_n - V_{\mathrm{bi}}) = -\Phi_B$ and $V(W) = -V_n - V$, where V_n is the potential between the electron transport and the Fermi level in the n layer. $n_e(0)$ at the metal/i layer interface can be calculated from the condition that zero current is flowing without voltage applied. $n_e(W)$ is equal to n_e in the n layer. $V(x)$ needed to integrate the left side is given by the usual Schottky approximation [16]. We obtain the usual diode characteristics,

$$J = J_0\left[\exp\left(\frac{qV}{f(T)}\right) - 1\right], \quad (5)$$

with a weakly voltage dependent saturation current J_0. By comparison with Eq. (1), the diode ideality factor n is given by the Einstein relation as $n = f(T)/kT$. Further calculations yield for the saturation current

$$J_0 \propto \mu \exp\left(\frac{q\Phi_B}{f(T)}\right). \quad (6)$$

A common characteristic of the deviations from the classical Einstein relation mentioned above is that the function $f(T)$ becomes temperature independent at sufficiently low temperatures. This situation has implications for the parameters n and J_0. First, the ideality factor should scale with $1/T$ as is, indeed, obtained for our diodes (cf. Fig. 3). Second, the thermal activation of J_0 is solely given by the temperature dependence of the mobility μ. Field-effect measurements of a doped n-ZnPc layer (doping ratio 1:41) yield an activation energy of 0.34 eV for the mobility, which is comparable to the slopes of $\ln J_0$ vs $1/T$ for both diodes (0.34 eV). The evident similarities of the parameters for M-i-n and p-i-n diodes indicate that the latter is likewise described by a diffusion-limited theory [20], rather than Shockley theory.

In summary, thin films of ZnPc doped with $[\mathrm{Ru(terpy)_2}]^0$ have been fabricated by the coevaporation technique in high vacuum. Electrical measurements show n-type conductivity of 2.7×10^{-6} S/cm at room temperature. ZnPc based p-i-n homojunctions and M-i-n diodes using $[\mathrm{Ru(terpy)_2}]^0$ as the n dopant has been successfully fabricated. The diodes show deviations from the classical models, which can be explained by deviations from the Einstein relation in the framework of diffusion theory. Although such deviations are commonly accepted, a general model that can properly describe the nature of disordered systems is not established yet. We hope to stimulate further research into the peculiarities of organic diodes and a more rigorous understanding of the properties of such junctions.

We thank S. Baranovskii (University of Marburg) for helpful discussions and the DFG (Leibniz grant) and NSF (CHE 0139637) for support.

Note added.—Recently we made another homojunction with wide-gap interlayer between ITO and p-ZnPc, having better film forming properties. We again observe strongly increasing n with decreasing temperature. While the I-V data still give a low value for Φ_B at low temperature, the barrier approaches the value obtained from C-V at higher temperatures. This confirms that the deviations from the Einstein equation are most pronounced at low temperature when localization effects dominate.

---

[1] M. Maitrot *et al.*, J. Appl. Phys. **60**, 2396 (1986); L. Athouel *et al.*, J. Chim. Phys. Phys.-Chim. Biol. **89**, 1279 (1992); P. Trouillas, A. Moliton, and B. Ratier, Synth. Met. **73**, 145 (1995).
[2] M. Pfeiffer *et al.*, Appl. Phys. Lett. **73**, 3202 (1998).
[3] B. Maennig *et al.*, Phys. Rev. B **64**, 195208 (2001).
[4] K. Yamashita *et al.*, Jpn. J. Appl. Phys. **34**, 3794 (1995); S. Hamm and H. Wachtel, J. Chem. Phys. **103**, 10 689 (1995); Q. Pei *et al.*, Science **269**, 1086 (1995).
[5] W. Shockley, Bell Syst. Tech. J. **28**, 435 (1949).
[6] C. van Berkel *et al.*, J. Appl. Phys. **73**, 5264 (1993); M. A. Kroon and R. A. C. M. M. van Swaaij, J. Appl. Phys. **90**, 994 (2001).
[7] M. Pfeiffer *et al.*, Org. Electron. **4**, 21 (2003); D. Gebeyehu *et al.*, Sol. Energy Mater. Sol. Cells **79**, 81 (2003).
[8] G. He *et al.*, Appl. Phys. Lett. **85**, 3911 (2004).
[9] A. Nollau *et al.*, J. Appl. Phys. **87**, 4340 (2000); A. G. Werner *et al.*, Appl. Phys. Lett. **82**, 4495 (2003); A. G. Werner *et al.*, Adv. Funct. Mater. **14**, 255 (2004).
[10] C. J. Bloom *et al.*, J. Phys. Chem. B **107**, 2933 (2003).
[11] Redox potentials can be related to an absolute energy scale by 0 V vs $\mathrm{Ag/Ag^+} = 4.7$ eV; see A. Bard and L. R. Faulkner, *Electrochemical Methods* (Wiley, New York, 2001).
[12] D. E. Morris, K. W. Hanck, and M. K. DeArmond, J. Electroanal. Chem. **149**, 115 (1983).
[13] D. Schlettwein *et al.*, J. Phys. Chem. B **105**, 4791 (2001).
[14] J. Blochwitz *et al.*, Org. Electron. **2**, 97 (2001).
[15] D. Gebeyehu *et al.*, Sol. Energy Mater. Sol. Cells **79**, 81 (2003).
[16] S. M. Sze, *Physics of Semiconductor Devices* (Wiley, New York, 1981), 2nd ed., p. 258.
[17] N. W. Ashcroft and N. D. Mermin, *Solid State Physics* (Saunders College Publishing, Fort Worth, 1976), p. 612.
[18] Y. Roichman and N. Tessler, Appl. Phys. Lett. **80**, 1948 (2002).
[19] R. Richert, L. Pautmeier, and H. Bässler, Phys. Rev. Lett. **63**, 547 (1989); S. D. Baranovskii *et al.*, Phys. Status Solidi B **205**, 87 (1998).
[20] K. Taretto, U. Rau, and J. H. Werner, Appl. Phys. A **77**, 865 (2003).